ChemComm

Cite this: *Chem. Commun.*, 2012, **48**, 10216–10218

www.rsc.org/chemcomm

COMMUNICATION

Cathode photoelectrochemical sensing of copper(II) based on analyte-induced formation of exciton trapping†

Peng Wang, Xiuyuan Ma, Mengqi Su, Qing Hao, Jianping Lei* and Huangxian Ju*

Received 3rd August 2012, Accepted 26th August 2012
DOI: 10.1039/c2cc35643k

The analyte-induced formation of exciton trapping leads to the decrease of cathode photocurrent of mercapto-capped CdTe quantum dots (QDs), which produces a sensitive cathode photoelectrochemical method for selective sensing of trace Cu^{2+} as the analyte with a linear range from 0.06 to 100 μM.

Photoelectrochemical analysis as a newly developed technology has drawn growing interest in many research fields,[1] such as cytosensing,[1a] immunoassay,[1b] and DNA analysis.[1c–e] These analytical methods are usually based on photocurrent enhancement *via* hole oxidation,[1f] dye-sensitization,[1g] and energy transfer,[1h] or photocurrent decrease *via* blocking of electron transfer.[2] All these processes are related to the presence of analytes. For example, when the photocurrent is produced *via* hole oxidation, the analyte can act as the electron donor to reduce the produced hole, which increases the photocurrent.[1g] In this process, the analyte can be considered as a sacrificial reagent. The electron blocking mechanism is often used in immunoassay, in which the formation of immunocomplex enhances steric hindrance, thus blocks the electron transfer. In order to improve the sensitivity of the immunoassay, the electron transfer resistance has been greatly enhanced by the precipitation of oxidation product catalyzed by enzyme labelled to secondary antibody.[2a] Another route to affect the analyte-related photocurrent is through the interaction between the nanoparticles immobilized on the electrode and the analyte,[2b] which produces an intermediate to disrupt the electron transfer from the conduction band of nanoparticles to the electrode. This route is efficient for the detection of copper ions by anodic photoelectrochemistry.

Compared with anode photoelectrochemical sensing, cathode sensing possesses some advantages such as less independence of the electron donor and stronger ability of anti-interference from reductive agents coexisting in biological samples. This technology can provide a supplementary platform for sensing applications. The different generating mechanism from anode photocurrent is also interesting in design of photoelectrochemical strategies. However, traditional photoelectrochemical substrates such as TiO_2, ZnO, and CdS have not been used as cathode materials for preparation of photoelectrochemical sensors and solar devices due to their high reduction overpotential. Recently, two cathode photoelectrochemical methods for detection of glucose have been reported using CdSe/ZnS and 3-mercapto-propionic-capped CdTe QDs, since these QDs can produce photocurrent at low cathode potentials.[3] Our previous work observed the strong cathodic electrochemiluminescent (ECL) emission of meso-2,3-dimercaptosuccinic acid capped CdTe quantum dots (DMSA-CdTe-QDs) at relatively low reduction overpotential and concluded that the unpassivated surface of QDs produced low surface energy level and narrow band gap, which made the surface electron transfer easier.[4] Under light excitation the electron transfer leads to the formation of an exciton.[5] The exciton can release a negatively charged electron into the vacant conduction band and leave an orbital hole in the valence band. This has been used for design of a cathode photoelectrochemical strategy based on the charge recombination suppression by the analyte as an electron donor to enhance the photoelectric conversion efficiency.[6]

Both the formation and the annihilation of the exciton depend on the surface states of the QDs. Here a method for inhibiting the formation of an exciton was designed by the competition interaction of metal ion toward the dithiol stabilizer on DMSA-CdTe-QDs to form the surface exciton trapping and change the surface state (Scheme 1). Using Cu^{2+} as a model analyte, a route to produce analyte-induced exciton trapping sites was proposed. These trapping sites decreased the cathode photocurrent, leading to a sensitive method for trace Cu^{2+} detection.

The DMSA-CdTe-QDs were synthesized according to our method reported previously,[4a] and verified using UV-vis and photoluminescent spectra (Fig. S1 in ESI†). The cathode photoelectrochemical sensor was fabricated by casting 10 μL DMSA-CdTe-QDs solution onto the surface of an F-doped tin oxide (FTO) electrode, which was pre-cut and cleaned. The scanning electron microscopic (SEM) morphology of the QD film exhibited a uniform layer with the aggregate sizes less than 20 nm (Fig. S2 in ESI†). The decline in aggregation and the homogeneous surface structure are favourable for improving the photoelectric conversion efficiency.

At an applied potential of −0.2 V (*vs.* SCE), the QD modified FTO electrode showed a signal-on photocurrent

State Key Laboratory of Analytical Chemistry for Life Science, Department of Chemistry, Nanjing University, Nanjing 210093, P. R. China. E-mail: hxju@nju.edu.cn, jpl@nju.edu.cn; Fax: +86 25 83593593; Tel: +86 25 83593593

† Electronic supplementary information (ESI) available: Experimental details, characterization of QDs, optimal conditions, and the detection of hair sample. See DOI: 10.1039/c2cc35643k

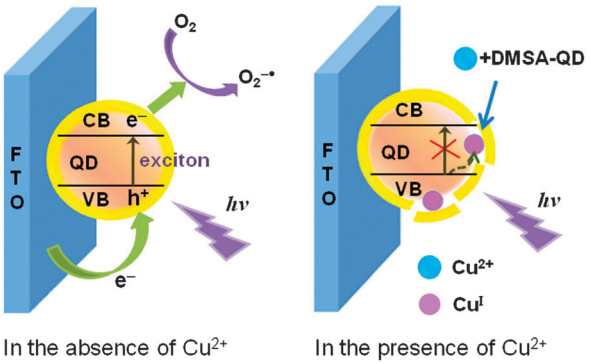

Scheme 1 Schematic illustration of exciton trapping mechanism and cathode photoelectrochemistry for sensing of Cu^{2+}.

response to irradiation with a wavelength of 405 nm (Fig. 1A, curve a). Upon the irradiation the photocurrent response increased by about 355 nA in an air-saturated buffer. After nitrogen gas was purged into the buffer continuously to decrease the oxygen content in the electrolyte, an obvious decrease of the photocurrent response was observed. After deoxygenation with nitrogen for 8 min, the photocurrent response became 18% of that measured in the air-saturated buffer (Fig. S3 in ESI†). These results indicated that O_2 participated in this photoelectrochemical process. Upon the irradiation, the exciton formed on the surface of the QDs released electrons into the vacant conduction band, which was then accepted by O_2 to produce $O_2^{-\bullet}$,[7] the orbital hole left in the valence band could obtain an electron from the FTO electrode at the cathode potential to produce a photocurrent.

The cathode photocurrent depended on the pH of the electrolyte (Fig. S4 in ESI†). In acidic solution, the QDs tended to decompose, resulting in a small photocurrent response. While at high pH the Cd^{2+} exposed at the surface defect sites would adsorb the OH^-, which hindered the electron transfer from QDs to O_2, and thus lowered the photocurrent. The maximum value of photocurrent response occurred at pH 6. Thus, pH 6.0 H_3BO_3-$Na_2B_4O_7$ buffer was used throughout the experiments.

The cathode photocurrent of the QD modified FTO electrode obviously decreased after adding Cu^{2+} (Fig. 1A). This could be attributed to the competition between Cu^{2+} and Cd^{2+} of QDs for S atoms in the DMSA molecule, since the sedimentation

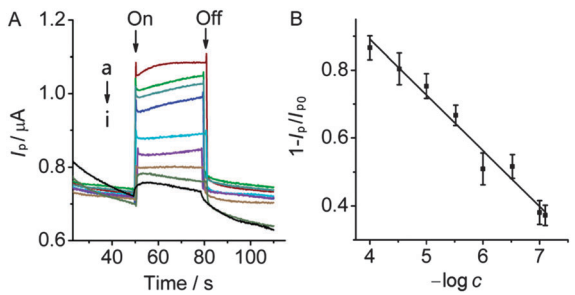

Fig. 1 (A) Cathode photocurrent responses of QD modified FTO electrode in an air-saturated buffer in the presence of 0, 0.08, 0.1, 0.3, 1.0, 3.0, 10, 30 and 100 μM Cu^{2+} (from a to i) at a bias potential of −0.2 V (*vs.* SCE) upon illumination. (B) Linear relationship between the response and Cu^{2+} concentration (n = 5). I_p and I_{p0} are photocurrent responses in the presence and absence of Cu^{2+}, respectively.

equilibrium constant of CuS (8×10^{-36}) is much smaller than that of CdS (7×10^{-27}),[8] indicating a stronger metal–S bond between copper and sulphur atoms than that between cadmium and sulphur atoms This interaction destructed the original Cd–S bond between DMSA and CdTe,[4b] leading to the partial decomposition of the QDs. Furthermore, the interaction between Cu^{2+} and the S atom led to a partial reduction of Cu^{2+}, providing the basis to form exciton trapping.

The reduction of Cu^{2+} on the QD surface and the formation of exciton trapping could be demonstrated with X-ray photoelectron spectroscopic (XPS) measurements. The Cd3d and Te3d XPS of QDs showed a Cd : Te molar ratio of about 8 : 1, suggesting most Cd^{2+} ions at the QD surface were stabilized by thiol ligands instead of Te atoms.[4b] After Cu^{2+} was added to the QD solution, this ratio became 3 : 1 (Fig. S5 in ESI†), indicating that more Te^{2-} ions were exposed and cupric ions were captured on the surface of CdTe QDs. Moreover, after interaction of Cu^{2+} with QDs, the binding energy of $Cu2p_{3/2}$ split into three parts with peak values of 931.4, 932.2, and 933.4 eV, respectively (Fig. 2). The peak at 933.4 eV represented the existence of Cu^{2+}, the peak at 931.4 eV resulted from Cu^{I}, while the peak at 932.2 eV could be attributed to the copper taking the form of Cu_xS at the mixed valence state. Generally, the form of the reduced copper can be expressed as CdS^+-Cu^+, in which the S comes from DMSA on the surface of the QDs. The redox energy level of Cu^{I} in CdS^+-Cu^+ species took place between the valance band and the conduction band of the QDs, resulting in the formation of the trapping sites.[9] The formed trapping sites resisted the formation of the exciton and thus the photoelectron and orbital hole, leading to the decrease of the cathode photocurrent response.

Based on the decrease of cathode photocurrent, the analyte-induced formation of exciton trapping could be used for the detection of Cu^{2+}. The plot of $1-I_p/I_{p0}$ *vs.* the logarithm of Cu^{2+} concentration showed a good linear relationship (Fig. 1B). The linear range was from 8.0×10^{-8} to 1.0×10^{-4} M with a detection limit (LOD) of 5.9×10^{-9} M calculated from 3σ. The average standard deviation gained from 5 independent experiments for all of the 8 concentrations was 6.5%, indicating good reproducibility and reliability of this method. The linear response range was wider than those based on fluorescence resonance energy transfer (0.16–2.87 μM),[10a] fluorescence quenching (0.008–2 μM),[10b] atomic absorption

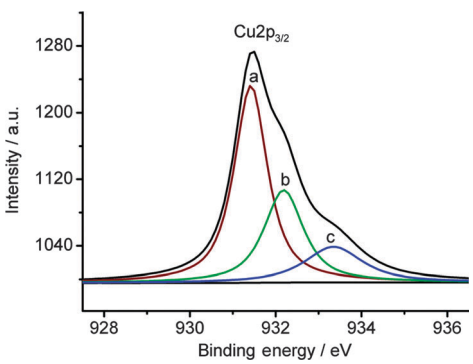

Fig. 2 XPS spectrum of Cu2p after the reaction of Cu^{2+} with QDs. The main peak was fitted into three sub-peaks at 931.4 (a), 932.2 (b), and 933.4 (c) eV.

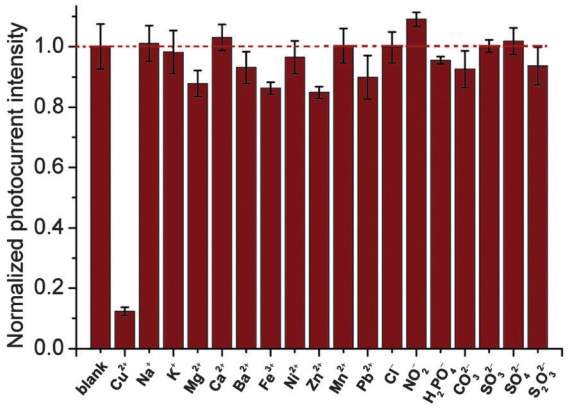

Fig. 3 Normalized photocurrent responses of QDs in the presence of 1×10^{-4} M individual ions.

(0.2–10 μM),[10c] voltammetric (0.075–2.5 μM),[10d] ECL (5.0 nM–7.0 μM),[4b] and anodic photoelectrochemical (0.02–20.0 μM)[2b] detection. The LOD was also lower than those of atomic absorption (0.2 μM),[10c] voltammetric (0.031 μM),[10d] and anodic photoelectrochemistric (0.01 μM)[2b] detections. The wide linear range and low LOD extended the practical application of the proposed method.

Different from the mechanism of anode photoelectrochemistry in the presence of Cu^{2+}, in which the formed Cu_xS competes for the electrons from the conduction band of the QDs with the electrode to decrease the photocurrent,[2b] here the formed Cu_xS was not an electron accepter, otherwise the cathode photocurrent would increase. Thus the decrease of cathode photocurrent resulted from the formation of Cu_xS or CdS^{+}-Cu^{+}, which acted as an exciton trap to decrease the photoelectric conversion efficiency. The analyte-induced formation mechanism of exciton trapping was obviously different from other cathode photoelectrochemical methods *via* electron transfer or charge recombination after exciton formation.[3,6] This process could efficiently reduce the interference in the detection of the real sample.

The interference of other ions was also examined. The majority of the anions such as Cl^-, NO_2^-, $H_2PO_4^-$, CO_3^-, SO_3^{2-}, SO_4^{2-} and $S_2O_3^{2-}$ did not interfere with the detection, and the interference of 1×10^{-4} M Na^+, K^+, Mg^{2+}, Ca^{2+}, Ba^{2+}, Fe^{3+}, Ni^{2+}, Zn^{2+}, Mn^{2+} and Pb^{2+} was also negligible (Fig. 3). Although 1×10^{-4} M Ag^+ interfered with the detection, 1×10^{-5} M Ag^+ did not show obvious photocurrent response. Meanwhile, Cu^{2+} and Ag^+ are not coexisting species in the majority of sceneries, including the samples from human hair, blood and body-liquid of the living creatures. Thus the proposed method possessed excellent ability against interference. Moreover, the detection could be performed at a low reduction potential, the reducing agents did not interfere with the cathode detection. Indeed, 1×10^{-4} M ascorbic acid did not change the photocurrent response.

To evaluate the analytical reliability and application potential of the proposed method, it was applied to detect the content of copper element in a human hair sample. The result showed a copper content of 13.4 μg g^{-1}, which was close to the value of 10.1 μg g^{-1} obtained from inductively coupled plasma (ICP) spectrometry (Table S1 in ESI†). The content of copper was well picked out among varieties of the other components, fitting well with the interfering ions test mentioned above.

In conclusion, DMSA-CdTe-QDs can produce sensitive cathode photocurrent response at a relatively low applied potential under illumination, which depends on the formation of exciton. Some analytes can interact with the QDs to form exciton trapping sites on QD surface and thus decrease the photoelectric conversion efficiency, which lowers the cathode photocurrent response. A novel cathode photoelectrochemical strategy has been designed for detection of trace Cu^{2+} based on the formation of analyte-induced exciton trapping. This proposed method has the advantages of wide linear range, low cost, easy fabrication, rapid response, high sensitivity and good selectivity. It can be successfully applied in the detection of copper in human hair sample. This work proposes a novel and promising route for photoelectrochemical sensing.

This work was financially supported by the National Basic Research Program (2010CB732400), and National Natural Science Foundation of China (21075060, 21135002, 21121091).

Notes and references

1 (*a*) Z. Qian, H. J. Bai, G. L. Wang, J. J. Xu and H. Y. Chen, *Biosens. Bioelectron.*, 2010, **25**, 2045–2050; (*b*) N. Haddour, J. Chauvin, C. Gondran and S. Cosnier, *J. Am. Chem. Soc.*, 2006, **128**, 9693–9698; (*c*) C. F. Ding, H. Li, X. L. Li and S. S. Zhang, *Chem. Commun.*, 2010, **46**, 7990–7992; (*d*) D. Baş and İ. H. Boyacı, *Anal. Bioanal. Chem.*, 2011, **400**, 703–707; (*e*) X. R. Zhang, Y. Q. Zhao, H. R. Zhou and B. Qu, *Biosens. Bioelectron.*, 2011, **26**, 2737–2741; (*f*) H. B. Li, J. Li, Q. Xu and X. Y. Hu, *Anal. Chem.*, 2011, **83**, 9681–9686; (*g*) W. W. Tu, Y. T. Dong, J. P. Lei and H. X. Ju, *Anal. Chem.*, 2010, **82**, 8711–8716; (*h*) W. W. Zhao, J. Wang, J. J. Xu and H. Y. Chen, *Chem. Commun.*, 2011, **47**, 10990–10992.

2 (*a*) W. W. Zhao, Z. Y. Ma, P. P. Yu, X. Y. Dong, J. J. Xu and H. Y. Chen, *Anal. Chem.*, 2012, **84**, 917–923; (*b*) G. L. Wang, J. J. Xu and H. Y. Chen, *Nanoscale*, 2010, **2**, 1112–1114.

3 (*a*) J. Tanne, D. Schäfer, W. Khalid, W. J. Parak and F. Lisdat, *Anal. Chem.*, 2011, **83**, 7778–7785; (*b*) W. J. Wang, L. Bao, J. P. Lei, W. W. Tu and H. X. Ju, *Anal. Chim. Acta*, 2012, DOI: 10.1016/j.aca.2012.07.025.

4 (*a*) X. Liu, L. X. Cheng, J. P. Lei and H. X. Ju, *Chem.–Eur. J.*, 2010, **16**, 10764–10770; (*b*) L. X. Cheng, X. Liu, J. P. Lei and H. X. Ju, *Anal. Chem.*, 2010, **82**, 3359–3364.

5 A. M. Smith and S. Nie, *Acc. Chem. Res.*, 2010, **43**, 190–200.

6 Q. Hao, P. Wang, X. Y. Ma, M. Q. Su, J. P. Lei and H. X. Ju, *Electrochem. Commun.*, 2012, **21**, 39–41.

7 (*a*) D. R. Cooper, N. M. Dimitrijevic and J. L. Nadeau, *Nanoscale*, 2010, **2**, 114–121; (*b*) Z. Xiong and X. S. Zhao, *J. Am. Chem. Soc.*, 2012, **134**, 5754–5757.

8 J. R. Goates, M. B. Gordon and N. D. Faux, *J. Am. Chem. Soc.*, 1952, **74**, 835–836.

9 Y. Chen and Z. Rosenzweig, *Anal. Chem.*, 2002, **74**, 5132–5138.

10 (*a*) P. Yang, Y. Zhao, Y. Lu, Q. Z. Xu, X. W. Xu, L. Dong and S. H. Yu, *ACS Nano*, 2011, **5**, 2147–2154; (*b*) W. B. Chen, X. J. Tu and X. Q. Guo, *Chem. Commun.*, 2009, 1736–1738; (*c*) J. F. Staden and C. J. Hattingh, *J. Anal. At. Spectrom.*, 1998, **13**, 23–28; (*d*) R. Takeuchi, A. Santos, P. Padilha and N. Stradiotto, *Talanta*, 2007, **71**, 771–777.